Coupling Efficiency of an Alignment-Tolerant, Single Fiber, Bi-Directional Link

S. C. Wang, J. Cross, S. M. Chai, A. Lopez, J. Park, M. A. Ingram, N. M. Jokerst, D. S. Wills, M. Brooke, and A. Brown

School of Electrical and Computer Engineering,
Georgia Institute of Technology,
Atlanta, GA 30332-0250

Abstract

In this paper, we present a novel Fourier technique to calculate the emitter-to-fiber coupling efficiency between an incoherent source of arbitrary directivity and a multimode fiber. The technique expresses the 4-D integral that describes the coupling as a 2-D sum, and along with Fourier series expansion, the technique increases greatly the computational speed of emitter-to-fiber coupling calculations. We have simulation results of the emitter-to-fiber coupling analysis and coupling analysis for a single-fiber bi-directional link total using the Fourier technique. The results show that the large core plastic optical fiber gives rise to good emitter-to-fiber coupling alignment tolerance, but tends to overfill the detector and cause degradation in fiber-to-detector alignment tolerance. We find that a more directive resonant-cavity light emitting diode only improves emitter-to-fiber alignment tolerance slightly, though it can couple more light into the fiber.

1. Introduction

For short haul (< 30 m), moderate speed (< 155 Mbps) communications with applications ranging from automotive wiring harness replacement [1] to local ATM cable links, cost becomes the dominant issue in the design of an optical fiber link. Low cost can be achieved through alignment tolerance in manufacturing and inexpensive components. In this paper, we consider a bi-directional optical link that incorporates large core plastic optical fiber (POF) and co-location of the emitter and the detector [2]. The silicon detector, which uses standard silicon CMOS, is large with a hole in the middle for the GaAs light emitting diode (LED), as shown in Fig. 1. The LED is placed in the hole using the well known epitaxial-lift-off method [3]. This co-located emitter-detector pair is surprisingly easy to manually align with inexpensive large core POF. We note that other bi-directional single-fiber designs require either the optoelectronic device (emitter /detector) to be biased differently to transmit or receive, or waveguide splitters to be used to separate the emitter and the detector at each end of the fiber [4]-[6]. The combination of co-location of the emitter and the detector, which eliminates the need for splitters, and the use of a single large core fiber, which provides good coupling alignment tolerance between the emitter and the fiber, leads to a low cost, bi-directional link design.

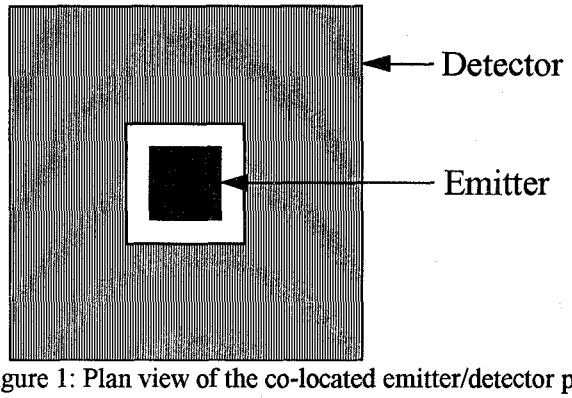

Figure 1: Plan view of the co-located emitter/detector pair.

Although the problem of coupling light from a light emitting diode (LED) into a large core fiber is well understood and is solved using geometrical optics [7,8], the time required to do the numerical integration in these calculations can be excessive when the objective is the optimization of LED and fiber parameters for an alignment tolerant design. In Section II, we summarize a novel technique [9] that formulates the geometrical optics treatment of emitter-to-fiber (EF) coupling as a convolution. The method can speed up the coupling calculation considerably compared to the brute force numerical integration method. In Section III, we present the results of EF coupling calculation using the new technique as a function of different key parameters such as emitter directivity and fiber core size. Our calculated data show excellent agreement with measured emitter-to-fiber (EF) coupling data. We also show results of a statistical alignment study of the bi-directional link, assuming a T. O. can-type connector design.

II. Analysis

Light that propagates into the fiber at an angle to the center axis of the fiber that is larger than the fiber numerical aperture angle, θ_{NA}, leaks out of the fiber through the cladding. More light is lost when there are longitudinal and

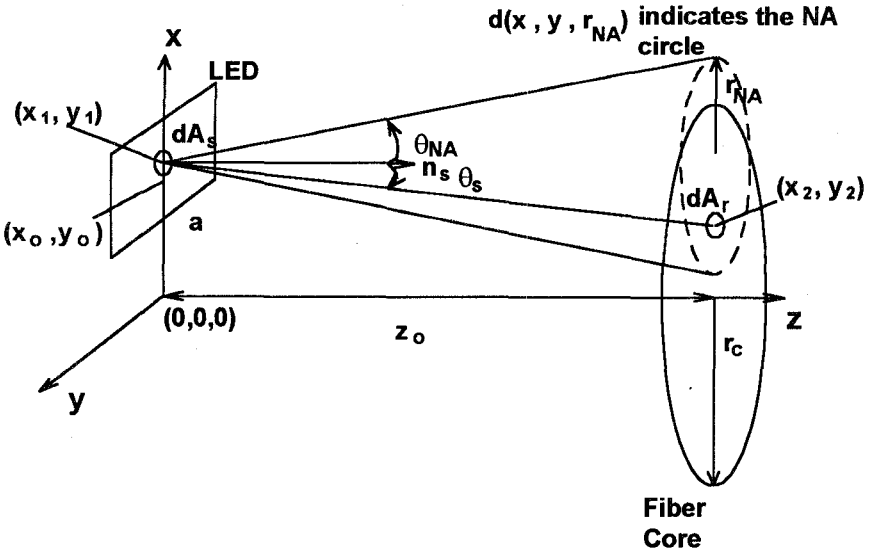

Figure 2: Geometry of coupling between the LED and the fiber with lateral and longitudinal misalignments.

lateral misalignments between the fiber and the LED. We begin by defining the geometry of the coupling problem when the LED and the fiber are misaligned as shown in Fig. 2. The z axis is the center axis of the fiber. The $z = 0$ plane contains the surface of the LED. The $z = z_o$ plane contains the input face of the fiber. We consider the distance z_o as the longitudinal misalignment between the fiber and the LED. The center of the LED has coordinates (x_o , y_o); these coordinates indicate the lateral misalignments. The circle with radius r_c and center $(0,0,z_o)$ outlines the circumference of the fiber core. The square with side length a outlines the emitter surface. The surface normal, $\mathbf{n}_s$, of the LED is parallel to the z axis. Since we consider the LED as an incoherent light source, we can first compute fiber coupling for a differential area dA_s. Then, we can obtain the total power coupled into the fiber by summing the contributions from all the differential areas of the emitter.

In the analysis that follows, we will consider the resonant-cavity light emitting diode (RCLED), which can be modeled as a somewhat directional but still incoherent source [10]. The radiance of the RCLED is given by

$$B(\theta_s) = B_o \cos^n(\theta_s), \tag{1}$$

where θ_s is the angle between the surface normal of dA_s and the line connecting $(x_1, y_1, 0)$ to (x_2 , y_2 , z_o), and n is the directivity of the source. $B(\theta_s)$ is the radiated power per unit source area, per unit solid angle, $d\Omega_s = \sin(\theta_s) d\theta_s \, d\phi_s$, in the direction specified by θ_s. Light rays from a differential source area can reach every point on the plane $z = z_o$. However, only those light rays arriving at plane $z = z_o$ with θ_s less than the numerical aperture (NA) angle θ_{NA} can be coupled into the fiber. Furthermore, the fiber will only propagate those light rays that reach the fiber core. So, mathematically we can express the total coupled power, Φ, from the entire source into the fiber as a 4-D integral,

$$\Phi = \int_{\text{LED}} \int_{\substack{\text{NA,}\\ \text{Fiber Core}}} B_o \cos^n(\theta_s) d\Omega_s dA_s , \tag{2}$$

where we remind the reader with text that the limit on the inner integral has to satisfy the restriction set by both the fiber NA and core.

From Fig. 2, we see that the fiber NA restricts the amount of useful light from a differential source located at $(x_1 , y_1 , 0)$ to a cone of $0 < \theta_s < \theta_{NA}$, which projects a NA circle at the fiber plane with a center at (x_1 , y_1 , z_o) and a radius of $r_{NA} = z_o \tan(\theta_{NA})$, whose circumference is outlined by dashed lines. The number of light rays that the fiber actually accepts is proportional to the overlap between the NA circle and the fiber. Therefore, we can express the limits of the inner integral in terms of the overlap between the NA circle and the fiber core. In order to do that, we have to change the inner integral over differential solid angle $d\Omega_s$ to differential area on the fiber plane. If we call (x_2 , y_2) the coordinates in the fiber plane, with the center of the fiber core as the origin, then the differential area on the fiber plane is just $dx_2 \, dy_2$, and the differential solid angle is equal to [11]:

$$d\Omega_s = dx_2 dy_2 \frac{\cos(\theta_s)}{R^2}, \tag{3}$$

where $R^2 = (x_2 - x_1)^2 + (y_2 - y_1)^2 + z_o^2$. Next, we write $\cos(\theta_s)$ as z_o / R, and we use the following disk function to represent the boundaries of the NA circle and the fiber core:

$$d(x,y,r) = \begin{cases} 1, & \sqrt{x^2 + y^2} \le r; \\ 0, & \text{otherwise,} \end{cases} \tag{4}$$

and the box function to represent the LED,

$$s(x,y)=\begin{cases}1, & |x|\le a/2 \text{ and } |y|\le a/2,\\ 0, & \text{otherwise.}\end{cases} \tag{5}$$

The result is a new expression for Eqn. 2

$$\Phi=\int\int dx_1dy_1s(x_1,y_1)\int\int dx_2dy_2\cdot \frac{B_o z_o^{n+1}}{R^{n+3}}d(x_1-x_2,y_1-y_2,r_{NA})\cdot d(x_2,y_2,r_c). \tag{6}$$

Observe that the inner integral of Eqn. 6 is in the form of a 2-D convolution. To see this, simply assign $f(x_1-x_2, y_1-y_2)$ and $c(x_2, y_2)$ to the first and the second terms in the inner integral, respectively, and Eqn. 6 becomes

$$\Phi=\int\int s(x_1,y_1)\big(f(x_1,y_1)*c(x_1,y_1)\big)dx_1dy_1 \tag{7}$$

Since d, s, f have finite domains, we can compute Eqn. 7 using an equivalent Fourier series expansion of the functions. As we shall see, the use of Fourier series greatly simplifies and speeds up the calculations. Let $\tilde{c}$, $\tilde{f}$, and $\tilde{s}$, be the periodically-extended versions of c, f, and s, respectively, with square period of side length W. Then, provided that this square period covers an area that is larger than both the core and the domain of the function that results from convolving f and c, Eqn. 7 can be expressed as

$$\Phi=\iint\limits_{\le|W/2|} dx_1dy_1\tilde{s}(x_1,y_1)\cdot \iint\limits_{\le|W/2|}\tilde{c}(x_2,y_2)\tilde{f}(x_1-x_2,y_1-y_2)dx_2dy_2. \tag{8}$$

Using Fourier series theory, we can rewrite Eqn. 8 in terms of the series coefficients of $\tilde{c}$, $\tilde{f}$, and $\tilde{s}$. The Fourier series representation of $\tilde{c}$ is [12]

$$\tilde{c}(x,y)=\sum_k\sum_l\tilde{C}(k,l)\exp\left[j\frac{2\pi(kx+ly)}{W}\right], \tag{9}$$

and the formula for the coefficients is

$$\tilde{C}(k,l)=\frac{1}{W^2}\int_{-\frac{W}{2}}^{\frac{W}{2}}\int_{-\frac{W}{2}}^{\frac{W}{2}}dxdy\;\tilde{c}(x,y)\exp\left[-j\frac{2\pi(kx+ly)}{W}\right]. \tag{10}$$

By expanding $\tilde{f}$, and $\tilde{s}$ in the same way, we have

$$\Phi=\sum_k\sum_l W^4\tilde{C}(k,l)\tilde{S}(k,l)\tilde{F}(k,l)\cdot \exp\left[-j\frac{2\pi(kx_o+ly_o)}{W}\right], \tag{11}$$

where we used the orthogonality principle of the basis functions of the Fourier series expansions. Now, all we need for the coupling calculation are the Fourier series coefficients of the fiber core, the NA circle, and LED, or $\tilde{C}$ and $\tilde{F}$, and $\tilde{S}$, respectively. The expression for the coefficients for the core and the LED can be found explicitly. The core coefficients can be calculated using

$$\tilde{C}(k,l)=\frac{r_c J_1\left(\frac{2r_c}{W}\sqrt{k^2+l^2}\right)}{W\sqrt{k^2+l^2}}, \tag{12}$$

where J_ν is the Bessel function of the first kind of the νth order. The LED coefficients can be calculated using

$$\tilde{S}(k,l)=\frac{\sin\left(\frac{a}{W}\pi k\right)}{\pi k}\frac{\sin\left(\frac{a}{W}\pi l\right)}{\pi l}. \tag{13}$$

Unlike the other coefficients, the coefficients of the NA circle must be integrated numerically. Fortunately, we will show that the integration needs to be performed only once for different values of lateral and longitudinal misalignments; therefore, the computing time needed to do analysis of sensitivity to misalignment is shortened by orders of magnitude. The coefficients of $\tilde{F}$ are

$$\tilde{F}(k,l)=\frac{2\pi}{W^2}\int_0^{r_{NA}}\frac{B_o z_o^{n+1}}{\sqrt[n+3]{r^2+z_o^2}}\cdot J_o\left(\frac{2\pi r}{W}\sqrt{k^2+l^2}\right)dr. \tag{14}$$

We observe that the above integral depends on longitudinal misalignment z_o. The procedure that we follow to eliminate that dependence has two steps. The first step consists of normalizing the dimension variables shown in Fig. 2 by z_o. We denote the normalized dimension variables with the

addition of an apostrophe. Some examples of the new dimensions are $r'_{NA} = \tan(\theta_{NA})$ and $W' = W/z_o$. To provide insight into this normalization, consider the following geometrical argument. Referring back to Fig. 2, we see that only the NA circle changes with z_o ; the LED area and the fiber core do not change with z_o . Therefore, instead of considering different sizes of NA circle (i.e. each different z_o), we will let the NA circle stay the same size and change the sizes of the LED and the fiber core such that the relative sizes remain the same. In the second step, we assign a fixed value for W', which means the ratio between W and z_o stays the same. We do this to ensure that the NA circle never extends outside of the W' square, regardless of the value of z_o . By following the procedure detailed above, $\widetilde{F}$ becomes independent of the longitudinal misalignment. The lateral misalignments do not affect $\widetilde{F}$ directly. However, they do play a major role in determining the value of W' because they determine the position of the LED with respect to the fiber core. Since we normalize the dimensions by z_o , a' , r_c' , x_o' , and y_o' increase when z_o decreases. We must make sure that for the smallest value of z_o that we are interested in, W' is large enough such that, no aliasing will result from using the Fourier series representation. Another factor that affects the accuracy of this technique is the number of terms needed in the sum of Eqn. 11. Both the size of W' and the number of terms needed are discussed in detail in [9].

III. Results

In this section, we present the bi-directional alignment study results obtained using the Fourier technique. We express the results in terms of an emitter-to-fiber (EF) alignment loss factor, η_{EF} ,

$$\eta_{EF} = \frac{\text{Power Coupled with Misalignment}}{\text{Power Coupled without Misalignment}}, \qquad (15)$$

and a fiber-to-detector (FD) alignment loss factor, η_{FD} ,

$$\eta_{FD} = \frac{\text{Power Intercepted by the Detector with Misalignment}}{\text{Power Radiated from the Fiber}}. \qquad (16)$$

The computation of η_{FD} is straightforward for a step-index fiber. Fig. 3 shows that the cone of light emitted from the fiber that does not overlap the detector is lost. Because of the hole in the middle of the detector array, the value of η_{FD} is always less than one. The total bi-directional loss factor is $\eta_{AL} = \eta_{EF} \times \eta_{FD}$.

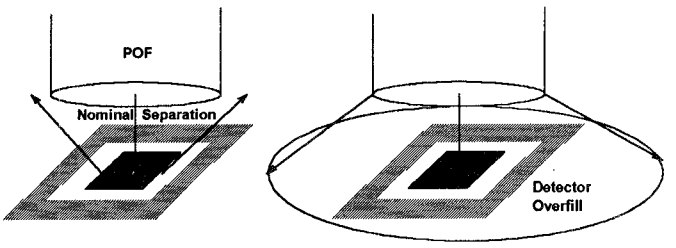

Figure 3: Experimental setup of a single fiber bi-directional link .

Our experimental setup, as shown in Fig. 3, consists of two integrated optoelectronic chips each having the following components:

1. A silicon detector in the shape of a square with a square hole in the middle with outer and inner side lengths of 1 mm and 0.3 mm, respectively, made up of an array of phototransistors.
2. A 0.15 mm x 0.15 mm thin film GaAs-based LED bonded directly into the center of the silicon detector array.
3. An interface chip that incorporates both digital circuitry and analog circuitry.

We use a 0.98 mm core POF as the link between the two chips and introduce misalignments with two XYZ stages.

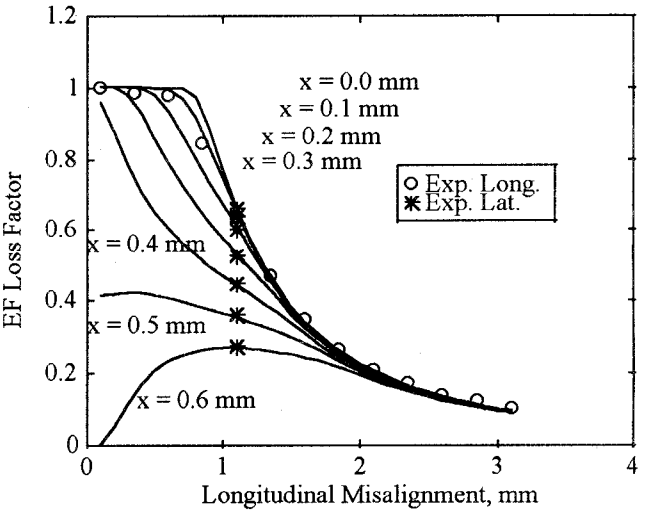

Figure 4: Theoretical and experimental EF loss values.

In Fig. 4, we plot in solid lines a family of calculated η_{EF} versus longitudinal separation for different lateral separations, using the experimental emitter and fiber parameters. We mark the lateral and longitudinal experimental results with "*" and "o" , respectively. The calculated and measured results show good agreement. These results also show that, when there is zero lateral misalignment, we can separate the fiber as far as 0.8 mm away from the emitter before any noticeable η_{EF} degradation occurs. With a longitudinal misalignment of 0.8 mm, we can displace the fiber as much as 0.4 mm laterally from the center of the emitter with less than a 3 dB η_{EF} degradation.

This alignment tolerance is due in large part to the 0.98 mm fiber core.

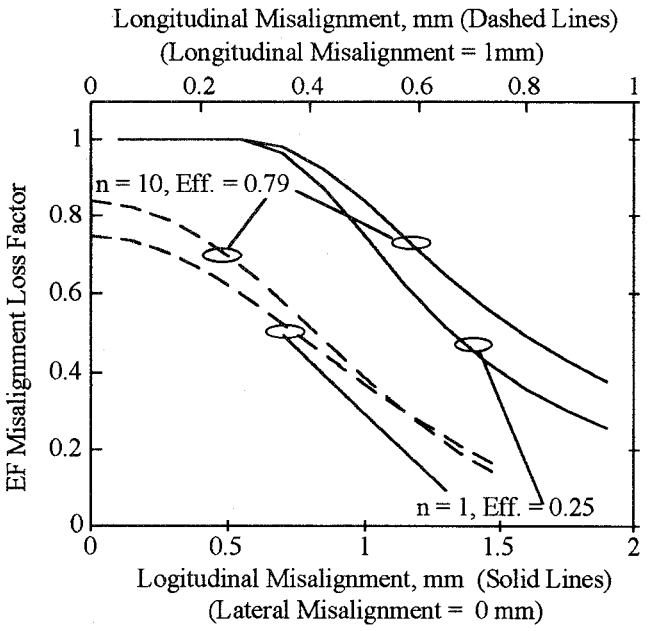

Figure 5 Comparison of longitudinal and lateral alignment tolerances between RCLED and LED.

In Fig. 5, we compare alignment results for a resonant-cavity light emitting diode (RCLED) with n = 10 [13] and a standard LED with n = 1. We plot η_{EF} versus longitudinal misalignments for zero lateral misalignment in solid lines (the x-axis values are labeled on the bottom of the graph) and η_{EF} versus lateral misalignment for longitudinal misalignment of 1.0 mm in dashed lines (the x-axis values are label on top of the graph). We see that the more directive RCLED improves longitudinal alignment and lateral alignment only slightly. Along with the values of n, we show on the graph the fraction of power from the emitter that is coupled into the fiber under zero (i.e. perfect) misalignment conditions, denoted by "Eff." The RCLED, with power spread out over a smaller range of solid angle, can couple 79% of its light into the fiber, while the standard LED can couple only 25% of its power into the fiber.

For bi-directional link performance, we have to consider not only the EF loss factor but also the FD loss factor. In connector design, there is often a nominal longitudinal separation. For example, a T. O. can-type connector, as shown in Fig. 6, requires enough separation between the chip and the glass for wire bonds and a fiber stop to protect the fiber from the glass. In Fig. 7, we plot the total alignment loss factor η_{AL} versus nominal longitudinal separation applied equally to both emitter and detector sides of the link. Different curves apply to different fiber core sizes. Observe that for a core radius of 0.5 mm, the loss factor degrades monotonically. This is because the diameter of largest core fiber is equal to the side length of the outer ring of the detector array, and the output from the fiber overfills the detector for any non-zero longitudinal separation, as shown in Fig. 3. Smaller core fibers have a non-zero optimal separation. For example, for a 0.3 mm core radius, the best nominal longitudinal separation is 0.35 mm. But for fibers whose core diameters are smaller than the side length of the inner ring of the detector array (fiber core radius < 0.167 mm), the light coming out of the fiber misses the detector entirely when there is zero longitudinal separation between the chip and the fiber.

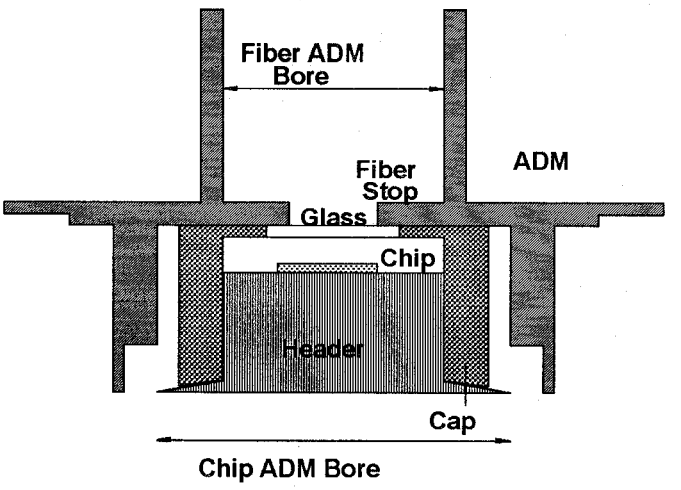

Figure 6: Schematic of a T. O. can-type connector. The nominal longitudinal separation between the O/E chip and the fiber is 0.8 mm.

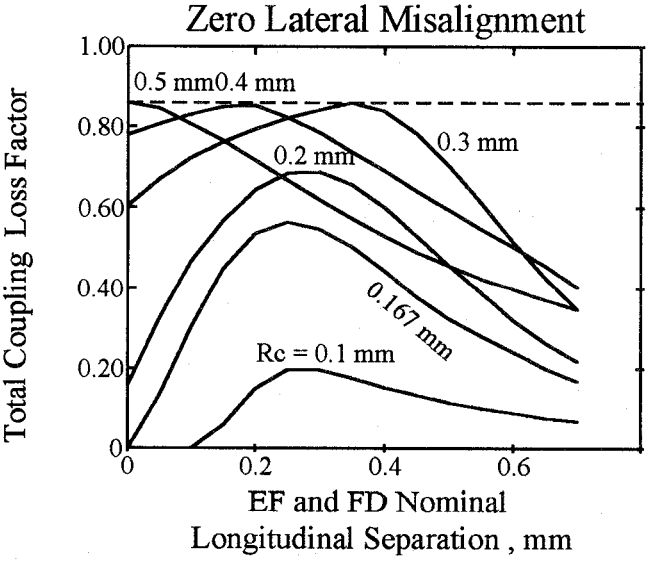

Figure 7 Plot of total coupling loss factor η_{AL} versus different nominal longitudinal separations between the emitter and the fiber and the detector and the fiber. Different fiber core radius are considered.

There are manufacturing tolerances associated with each dimension of a T. O. can-type connector. We have derived a

statistical model for EF and FD misalignments loosely based on these tolerances. Our model treats the longitudinal misalignment as a Gaussian random variable with mean 0.8 mm and σ = 0.0633 mm, and the lateral misalignment as the sum of a number of uniform and Gaussian independent random variables such that the sum has mean of 0 mm and σ = 0.1 mm. We have performed a Monte Carlo simulation of 500 random trials, and we show the simulation results in Figure 8. Case 1 results correspond to our experimental emitter, fiber, and detector parameters. The total alignment loss factor ranges from 4 to 7 dB for different misalignment conditions. We note that the mean longitudinal separation between the fiber and the emitter/detector pair for the model is located all the way to the right of the graph in Fig. 7. Most of the coupling loss is due to detector overfill. To improve the coupling loss factor, we can either decrease the nominal longitudinal separation, or we can increase the size of the detector. The effects of increasing the detector size are shown as Case 2 of Figure 8; for this case, the loss factor ranges from 1 to 4 dB.

IV. Conclusion

Using the conventional approach, an alignment study for the emitter-to-fiber misalignment requires a time-consuming 4-D numerical integration for each value of lateral and longitudinal misalignment. In the first part of the paper, we summarize a novel Fourier series approach for fast calculation of the coupling efficiency. The method formulates the geometrical optics treatment of emitter-to-fiber coupling as a convolution. Using a Fourier series representation of the source area, fiber core area, and the numerical aperture of the fiber, a misalignment between the emitter and the fiber becomes a phase shift on the Fourier coefficients, and the numerical integration simplifies into a sum that is about 3 orders of magnitude faster to compute. The gain in computational speed facilitates the study of design tradeoffs for the optoelectronics and the connectors. Using the Fourier technique, we have studied the alignment tolerance of our single fiber bi-directional link, in which we exploit the combination of the co-location of the emitter and detector and the alignment tolerance of large core plastic optical fiber to achieve low cost link design. We show that the emitter can be longitudinally misaligned as much as 0.8 mm without noticeable degradation in emitter-to-fiber coupling, and that when the emitter and fiber are 0.8 mm apart longitudinally, the emitter can be laterally misaligned as much as 0.4 mm with less than a 3 dB degradation. We have shown that the calculated emitter-to-fiber loss factor values agree with the measured values, and that a more directive resonant-cavity light emitting diode improves the emitter-to-fiber alignment tolerance only slightly. However, the more directive source can couple more light into the fiber. We have studied the total alignment loss factor for a bi-directional link using the Fourier technique. We have found that the overfilling of the detector gives rise to an optimal nominal longitudinal separation between the fiber and the emitter/detector pair. We have also performed a Monte Carlo simulation of misalignment of our link based on a T. O. can-type connector design. The results show that our proposed link has a mean total alignment loss factor of about 5 dB.

Acknowledgment

This work was supported by the Manufacturing Research Center and the Packaging Research Center of the Georgia Institute of Technology.

References

[1] M. A. Saifi, Y. Tsuji, G. Idei, and H. Ohuchi, "Emerging applications of optical fibers and optical technologies in automobiles, " *Proceedings of the SPIE*, vol. 1817, pp. 116-133, 1992.

[2] J. Cross, et al., " A Single Fiber Bi-Directional Optical Link Using Co-Located Emitters and Detectors,", *IEEE Photonics Technology Letters*, vol. 8, no. 10, pp.1385-88, October, 1996.

[3] C. Camperi-Ginestet, M Hargis, N. M. Jokerst, and M. Allen, " Alignable Epitaxial Liftoff of GaAs Materials with Selective Deposition Using Polyimide Diaphragms," *IEEE Photon. Tech. Lett.*, vol. 3, pp. 1123-6, 1991.

[4] J. Jauden, H. Porte, J.-P. Coedgebuer, J. Abiven, C. Gibassier, and C. Gutierrez-Martinez, "Polarization Independent Bidirectional Fiber Link Using Coherence Multi/Demultiplexing $LiNbO_3$ Integrated Electrooptical Circuits," *IEEE/OSA Jouranl of Lightwave Technology*, vol. 14, no. 7, July 1996.

[5] R. J. Orazi and M. N. McLandrich, "Bidirectional Transmission at 1.55 Microns using Fused Fiber Narrow Channel Wavelength Division Multiplexors and Erbium Doped Fiber Amplifiers," *IEEE Photon. Technol. Lett.*, vol. 6, no. 4, 571-4, 1994.

[6]N. J. Frigo, P. P. Iannone, P. D. Magill, T. E. Darcie, M. M. Downs, B. N. Desai, U. Koren, T. L. Koch, C. Dragone, H. M. Presby, G. E. Bodeep, "A Wavelength-Division Multiplexed Passive Optical Network with Cost-Shared Components," *IEEE Photon. Tech. Lett.*, vol. 6, pp. 1365-7, 1994

[7] K. H. Yang and J. D. Kingsley, "Calculation of Coupling Losses Between Light Emitting Diodes and Low-Loss Optical Fibers," *Applied Optics*, vol. 14, no. 2, pp.288-293, Feb. 1975.

[8] Joseph C. Palais, Fiber *Optic Communications*, New York:Prentice-Hall, Inc., 1992.
[9] Shih-Cheng Wang and Mary Ann Ingram, "A Novel Fourier Technique for Calculating Fiber-to-LED Coupling Efficiency with Misalignments," *IEEE/OSA Journal of Lightwave and Technology*, vol. 14, no. 10, October, 1996.

[10] M. Selim Ünlü and Samuel Strite, "Resonant Cavity Enhanced Photonic Devices," *Journal of Applied Physics*, vol. 78, no. 2, July 15, 1995.

[11] Frank L. Pedroti and Leno S. Pedrotti, *Introduction to Optics*, New York:Prentice-Hall, Inc., 1987.

[12] Dan E. Dudgeon and Russel M. Mersereau, *Multidimensional Digital Signal Processing*, New York:Prentice-Hall, Inc., 1984.

[13] Scott T. Wilkinson, Nan M. Jokerst, and Richard P. Leavitt, "Resonant-Cavity-Enhanced Thin-Film ALGaAs/GaAs/AlGaAs LED's with Metal Mirrors," *Applied Optics*, vol. 34, no. 36, pp. 8298-8302, December 1995.

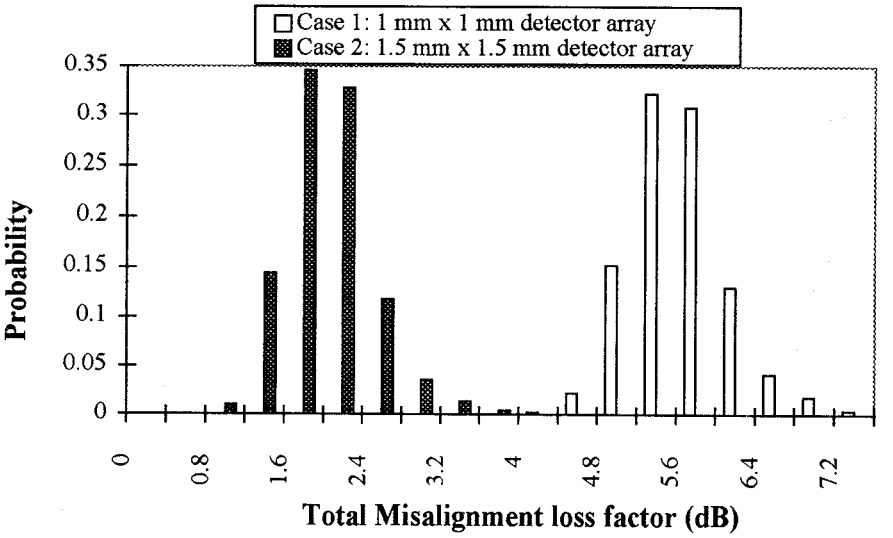

Figure 8: Monte Carlo simulation results of total misalignment loss for a T. O. can-type connector.